Article

Telomere-Driven Tetraploidization Occurs in Human Cells Undergoing Crisis and Promotes Transformation of Mouse Cells

Teresa Davoli[1] and Titia de Lange[1,*]
[1]Laboratory for Genetics and Cell Biology, The Rockefeller University, 1230 York Avenue, New York, NY 10065, USA
*Correspondence: delange@mail.rockefeller.edu
DOI 10.1016/j.ccr.2012.03.044

SUMMARY

Human cancers with a subtetraploid karyotype are thought to originate from tetraploid precursors, but the cause of tetraploidization is unknown. We previously documented endoreduplication in mouse cells with persistent telomere dysfunction or genome-wide DNA damage. We now report that endoreduplication and mitotic failure occur during telomere crisis in human fibroblasts and mammary epithelial cells and document the role of p53 and Rb in repressing tetraploidization. Using an inducible system to generate transient telomere damage, we show that telomere-driven tetraploidization enhances the tumorigenic transformation of mouse cells. Similar to human solid cancers, the resulting tumors evolved subtetraploid karyotypes. These data establish that telomere-driven tetraploidization is induced by critically short telomeres and has the potential to promote tumorigenesis in early cancerous lesions.

INTRODUCTION

Aneuploidy is a general feature of human solid tumors. An important source of aneuploidy is an elevated rate of chromosome mis-segregation (Lengauer et al., 1997). However, a substantial fraction of tumors have very high chromosome numbers, ranging from hypertriploid to subtetraploid, making it unlikely that nondisjunction of individual chromosomes is the sole mechanism responsible for their abnormal karyotypes (reviewed in Ganem et al., 2007; Storchova and Kuffer, 2008; Davoli and de Lange, 2011). More likely, these tumors arise from an initial tetraploidization event that is followed by frequent chromosome loss (Shackney et al., 1989). Indeed, tetraploid nuclei and supernumerary centrosomes have been noted in the early stages of some solid tumors (Reid et al., 1996; Kirkland et al., 1967). Importantly, tetraploidization after chemically induced cytokinesis failure has been shown to promote tumorigenesis in p53-deficient mouse mammary epithelial cells (Fujiwara et al., 2005).

Potential sources of tetraploidization in cancer are mutations in the tumor suppressor Adenomatous Polyposis Coli or deregulation of mitotic factors such as Mad2, Emi1, LATS1, and AuroraA (Davoli and de Lange, 2011). An additional mechanism for the duplication of cancer genomes was suggested by the frequent tetraploidization in mouse cells experiencing telomere dysfunction (de Lange, 2005; Hockemeyer et al., 2006; Davoli et al., 2010; Kibe et al., 2010). In these experiments, telomere dysfunction was induced by removing the shelterin proteins POT1a and POT1b from the telomeres of p53-deficient mouse embryo fibroblasts (MEFs). The resulting ataxia telangiectasia-and Rad3-related (ATR) signaling forestalls the activation of Cdk1/CyclinB, blocking entry into mitosis. However, after a prolonged period in G2, the replication inhibitor geminin is degraded and the licensing factor Cdt1 is re-expressed allowing the cells to re-enter S phase, resulting in endoreduplication. Endoreduplication and tetraploidy are also induced by continuous treatment of p53-deficient MEFs with genotoxic drugs, indicating that the endocycles are due to the persistence of the DNA damage signal rather than its origin.

We have proposed that the telomere-dependent pathway for tetraploidization is relevant to human cancer because telomere attrition is widespread during tumorigenesis (de Lange et al., 1990; Hastie et al., 1990; Meeker et al., 2002, 2004; van Heek et al., 2002; Meeker and Argani, 2004). Due to the absence of telomerase (Kim et al., 1994), telomeres shorten with cell

Significance

Tetraploidization can occur early in tumorigenesis and is thought to be responsible for the emergence of aneuploid cancer karyotypes with high chromosome numbers. Here, we show that tetraploidy is induced when human p53/Rb-deficient fibroblasts and mammary epithelial cells enter telomere crisis. Mouse cells that have become tetraploid after telomere dysfunction have an increased transformation potential. These findings can explain how tetraploidization occurs in human cancer and point to the importance of telomere dysfunction in shaping cancer genomes.

divisions in most human somatic cells, including cells undergoing the first stages of tumorigenic transformation. After extensive proliferation, dysfunctional short telomeres are recognized as sites of DNA damage by the ATM and ATR kinases and induce p53/Rb-mediated senescence or apoptosis (d'Adda di Fagagna et al., 2003; Herbig et al., 2004). In the absence of p53 and Rb function, cells continue to proliferate despite the presence of dysfunctional telomeres (Wright and Shay, 1992; Shay and Wright, 2005). Eventually, the cells enter telomere crisis, a stage in which the rampant genome instability associated with lack of telomere function curbs cell proliferation and survival (Wright and Shay, 1992; Shay et al., 1993; Shay and Wright, 2005; Counter et al., 1992).

There is mounting evidence that prior to the activation of telomerase, developing cancers can experience a period of telomere crisis (Meeker et al., 2004; de Lange, 2005). Molecular analysis of chronic lymphocytic leukemia has revealed evidence for telomere fusions, a product of telomere crisis (Lin et al., 2010). Furthermore, telomere crisis was inferred to occur in the ductal carcinoma in situ (DCIS) stage of breast cancer based on the presence of short telomeres and an abrupt rise in genome instability before telomerase is activated (Chin et al., 2004). Modeling in the mouse has provided evidence that the genome instability arising in telomere crisis can promote tumorigenesis in a permissive setting (Artandi and DePinho, 2010; Artandi et al., 2000).

Here, we investigate the frequency and mechanism of tetraploidization in human fibroblasts and epithelial cells undergoing telomere crisis. FUCCI imaging for geminin and Cdt1 revealed that tetraploidization was due to both mitotic failure and endoreduplication. Moreover, using mouse cells we show that tetraploidization-induced by telomere dysfunction can promote tumorigenesis, as is the case for tetraploidization induced by cytokinesis inhibitors (Fujiwara et al., 2005). The resulting tumors have a chromosome complement reminiscent of the subtetraploid karyotypes of human solid tumors. These data are consistent with a role for telomere dysfunction in the induction of tetraploidy in the early stages of human tumor development.

RESULTS

Tetraploidization in Telomere Crisis

To generate cells in telomere crisis, telomerase-negative human IMR90 and BJ fibroblasts were rendered p53- and Rb-deficient through expression of SV40 large T antigen (SV40-LT). As expected, the telomeres shortened progressively in these cultures (Figure 1A), resulting in telomere crisis at population doubling (PD) 80–90 for IMR90-SV40LT and at PD 105–110 for BJ-SV40LT. Telomere crisis was evident from the plateau in the growth curve (Figure 1B), the increased number of 53BP1 DNA damage foci (Figure 1C), and the phosphorylation of Chk1 and Chk2 (Figure 1D). Fluorescence-activated cell sorting (FACS) analysis showed that the fraction of tetraploid cells (estimated based on the fraction of cells with a DNA content >4N) progressively increased from 2%–3% at early PDs to 30%–35% at the time of telomere crisis (Figure 1E). Similarly, BJ fibroblasts transformed by HPV E6 and E7 displayed hallmarks of telomere crisis and accompanying tetraploidization at PD 90–100 (Figures S1A–S1D available online).

Telomere crisis was also induced in two telomerase-negative human mammary epithelial cell strains (hMECs), 184B-GSE22 and 48RS-GSE22, which lack a functional Rb pathway and express the p53 inhibitory peptide GSE22 (Romanov et al., 2001; Garbe et al., 2007). When these cells divide beyond senescence, they continue to erode their telomeres and enter a telomere crisis that is accompanied by genome instability (Romanov et al., 2001). The p53-proficient 184B and 48RS precursors were used as controls. The 184B-GSE22 and 48RS-GSE22 cultures entered telomere crisis at passage 18-20 and passage 28-32, respectively, showing shortened telomeres, an increase in the frequency of 53BP1 foci, and phosphorylation of Chk1 and Chk2 (Figures 2A and 2B; Figures S2A and S2B). FACS analysis showed an increase in the fraction of cells with >4N DNA content upon entry into telomere crisis in the two p53/Rb-negative hMEC cultures, whereas the parallel p53-proficient counterparts showed a G1/S arrest without tetraploidization (Figures 2C and 2D). Tetraploidization in telomere crisis was confirmed by analyzing the chromosome numbers of metaphase spreads (Figure S2C). The GSE-22 expressing hMECs, but not their p53-proficient counterparts, showed evidence for tetraploidization when precrisis cultures were treated with zeocin for 96 hr (Figures 2E and 2F).

Thus, in epithelial cells as well as in fibroblasts, telomere crisis and prolonged genome-wide DNA damage is accompanied by polyploidization resulting in tetraploid cells. While the formation of tetraploid cells is readily demonstrable, we note that the 8N peak in the FACS profiles of cells in crisis could represent octoploid cells in G1 as well as tetraploid cells in G2. As two successive aberrant cell cycles are required to generate octoploid cells, octoploidization might be too infrequent to result in a clear 16N peak in the FACS profiles.

Endoreduplication and Mitotic Failure in Telomere Crisis

The increased ploidy of cells in telomere crisis could be due to either endoreduplication or a failure in the late stages of mitosis, since dicentrics formed by telomere fusions (Figure S2D) hinder the completion of cytokinesis. To distinguish between these events, we performed live-cell imaging using the FUCCI system (Sakaue-Sawano et al., 2008), which previously demonstrated endoreduplication in POT1a/b DKO cells (Davoli et al., 2010). FUCCI is based on the cell cycle dependent expression of fluorescently tagged fragments of Cdt1 and geminin. The licensing factor Cdt1, which mediates the formation of prereplication complexes, is expressed in G1 and degraded upon entry into S phase in a process that is coupled to DNA replication (Arias and Walter, 2005; Remus and Diffley, 2009). Cdt1 is further inhibited by geminin, which is expressed in S/G2. In a normal mitotic cycle, geminin is degraded during mitosis, thereby reestablishing a state that is permissive to origin licensing in the daughter cells. However, in cells undergoing telomere-driven endoreduplication, geminin degradation takes place in the absence of mitosis, allowing cells to enter a G1-like state in which Cdt1 can mediate a second round of DNA replication. Thus, mitosis-independent geminin degradation is an indicator for endoreduplication (Figures 3A and 3B; Movie S1). In addition, FUCCI imaging can be used to detect mitotic failure based on the breakdown of the nuclear envelope that signifies entry into mitosis and
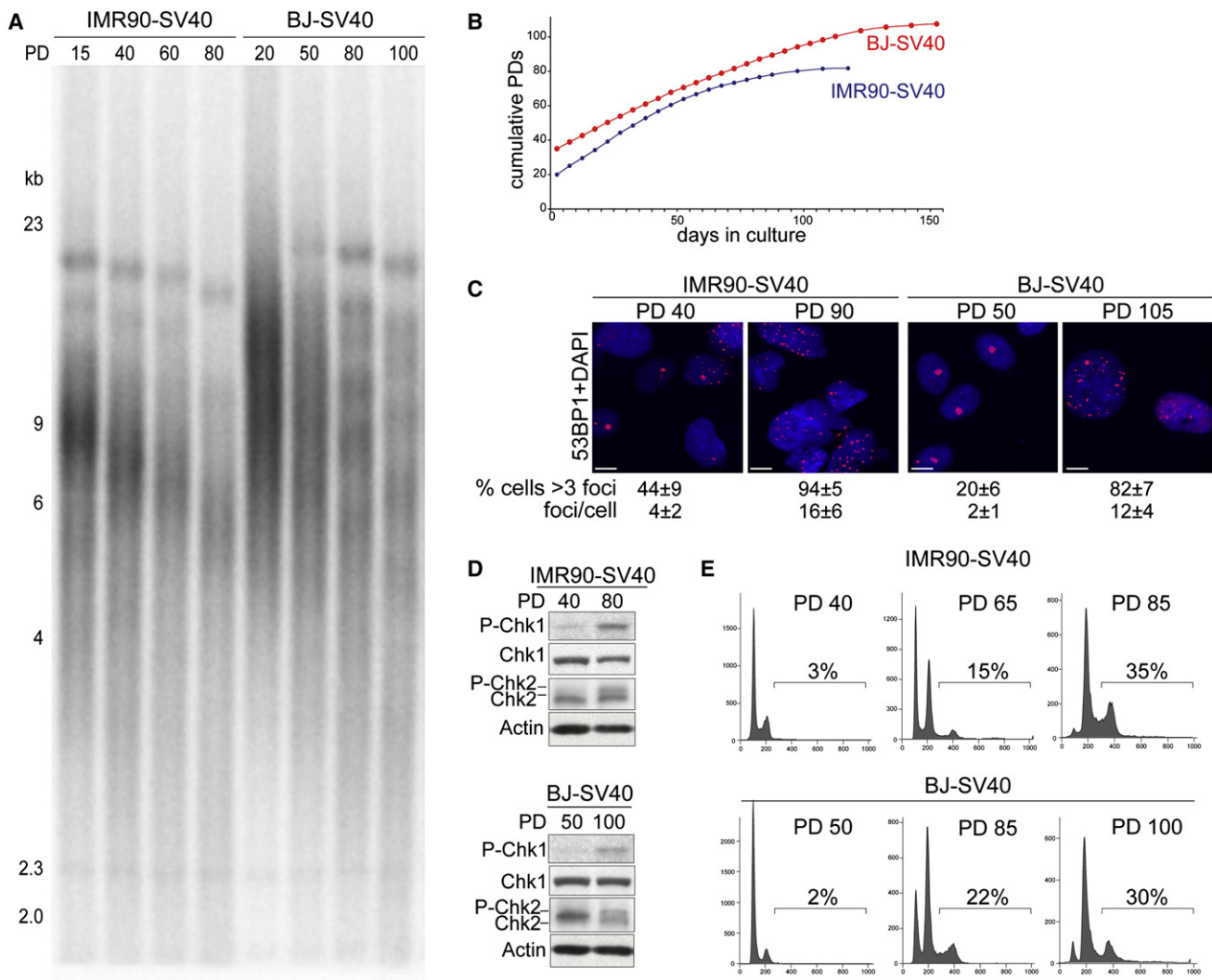
Figure 1. Tetraploidization of BJ-SV40 and IMR90-SV40 in Telomere Crisis

(A) Genomic blot for telomere restriction fragments of SV40-LT transformed IMR90 and BJ human fibroblasts at the indicated PD.

(B) Growth curve of IMR90-SV40 and BJ-SV40 from PD 20 or 38, respectively, until crisis (105–110 PDs for BJ-SV40 cells and at 80–90 for IMR90-SV40).

(C) IF analysis of 53BP1 foci in the cells at the indicated PDs. The average number of 53BP1 foci per cell and the percentage of cells with more than three foci are shown with SD. Scale bar = 5 μm.

(D) Immunoblots for P-Chk1 and P-Chk2 in the BJ-SV40 and IMR90-SV40 cells at the indicated PD.

(E) FACS profiles (PI staining) of IMR90-SV40 and BJ-SV40 cells indicated PD. The percentage of cells with >4N DNA content is indicated.

See also Figure S1.

the binucleated or multinucleated cells that result from a failure in cytokinesis (Figures 3A and 3B; Movie S1).

As expected, FUCCI imaging at early PDs (PD < 50) of BJ-SV40 and BJ-E6/E7 fibroblasts showed that in most cells geminin degradation coincided with mitosis, whereas endocycles and mitotic failure were rare (<5%) (Figures 3A–3C; Movie S1). However, at the late PDs when the cells entered telomere crisis, the fraction of BJ-SV40, BJ-E6E7 and IMR90-SV40 cells undergoing geminin degradation in the absence of mitosis increased to 12%–17% (Figures 3A–3C; Figure S3; Movies S1 and S2). After loss of geminin, most of these cells expressed Cdt1 and entered a second S phase as deduced from the degradation of Cdt1 and reappearance of geminin. During these endocycles

there was no evidence of nuclear envelope breakdown. The BJ-SV40 fibroblasts in telomere crisis also displayed a prolonged S/G2 phase whereas G1 was only minimally affected (Figure 3D; Movie S1). In addition, the cells showed occasional metaphase spreads with diplochromosomes, a characteristic consequence of endoreduplication representing duplicated sister chromatids that are held together by the centromeric cohesin (Figure S2D).

In addition to endoreduplication, fibroblasts in telomere crisis showed a considerable level of mitotic failure (Figures 3A–3C; Figure S3; Movies S1 and S2). Their aberrant mitosis was presumably due to the dicentric chromosomes resulting from telomere fusions (Figure S2D). The cells attempted mitosis as
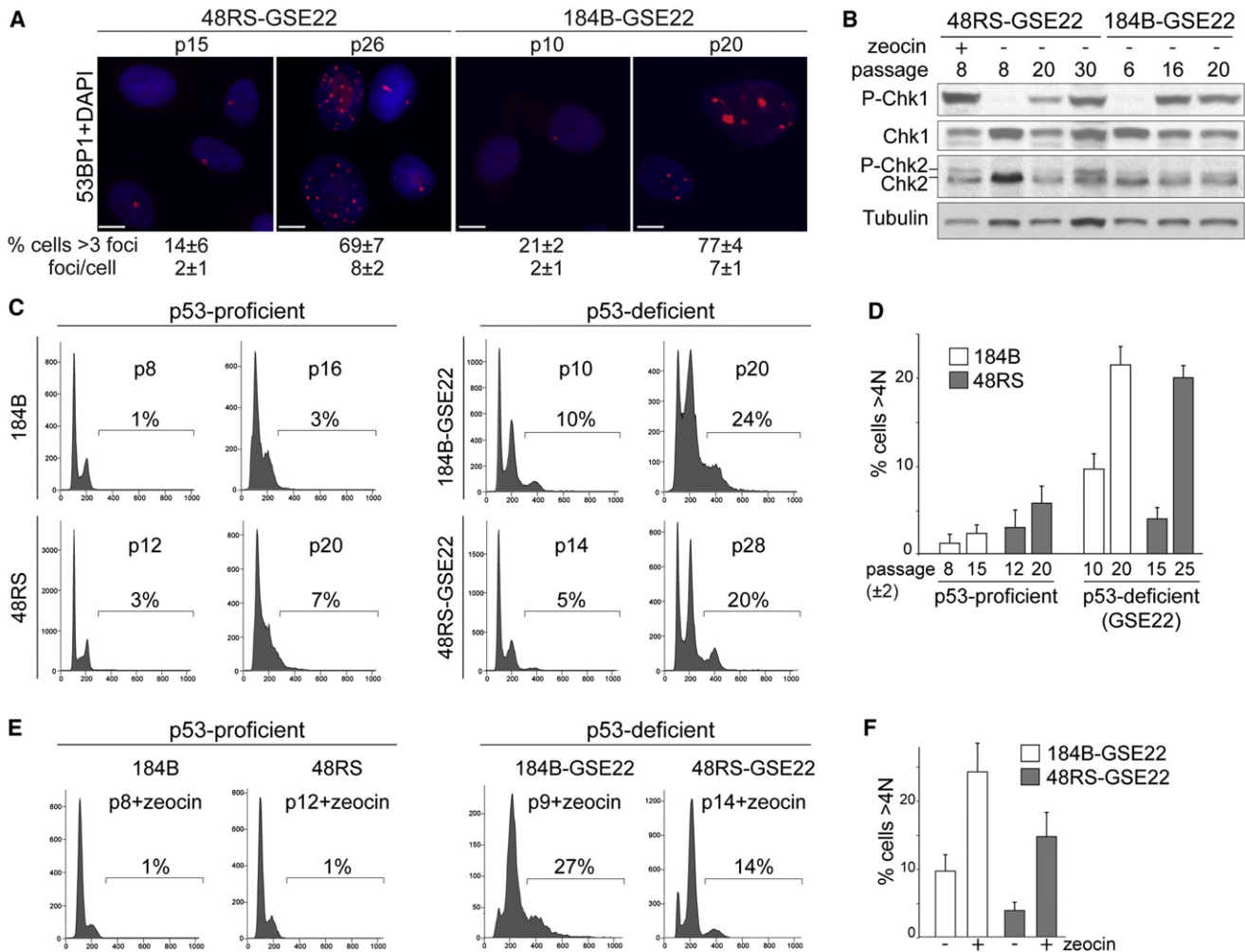
Figure 2. Tetraploidization of hMECs in Telomere Crisis

(A) IF for 53BP1 foci in 184B-GSE22 and 48RS-GSE22 hMECs at the indicated passage. The average number of 53BP1 foci per nucleus and the percentage of cells with more than three foci are given with standard deviation. Scale bar = 5 μm.

(B) Immunoblots for Chk1 and Chk2 phosphorylation in 48RS-GSE22 and 184B-GSE22 at the indicated passage and after zeocin treatment.

(C and D) FACS analysis of the indicated hMECs at the indicated passage. The percentage of cells with DNA content >4N is indicated. Quantification of averages of two or three independent experiments is shown in (D).

(E and F) FACS analysis of 184B-GSE22 and 48RS-GSE22 at the indicated (early) passage treated with zeocin. The percentage of cells with a DNA content >4N is indicated. Quantification of three independent experiments is shown in (F).

See also Figure S2.

evidenced by their rounding up and breakdown of the nuclear envelope leading to the presence of geminin throughout the cells. However, the execution of cytokinesis appeared to fail, resulting in binucleated or multinucleated cells (Movies S1 and S2).

Endoreduplication and mitotic failure was also observed in the hMEC lines 48RS-GSE22 and 184B-GSE22 in telomere crisis and upon continuous treatment with zeocin (Figures 4A and 4B; Movie S3). Mitotic failure appeared to be more frequent in the hMECs compared to the BJ and IMR90 fibroblasts. For instance, in the presence of zeocin, BJ-SV40 fibroblasts predominantly show endoreduplication, whereas hMECs also show mitotic failure events (Figures 4A and 4B; Movie S3; Davoli et al., 2010; data not shown).

Role of Rb in Blocking Telomere-Driven Tetraploidization

In human cells, activation of the Rb pathway contributes to the cell cycle arrest in response to a genome-wide or telomere-derived DNA damage signal (Jacobs and de Lange, 2004; Shay et al., 1991; Smogorzewska and de Lange, 2002; Shay and Wright, 2005). In order to determine whether the Rb pathway can block tetraploidization, we analyzed telomerase-negative BJ fibroblasts with an unaltered Rb pathway. The p53 dominant-negative allele (p53 dn, p53175H) was used to abrogate the p53 response to DNA damage (p53 dn, Baker et al., 1990; Jacobs and de Lange, 2004).

To measure their propensity for tetraploidization, the BJ-p53 dn cells were either subjected to continuous zeocin treatment
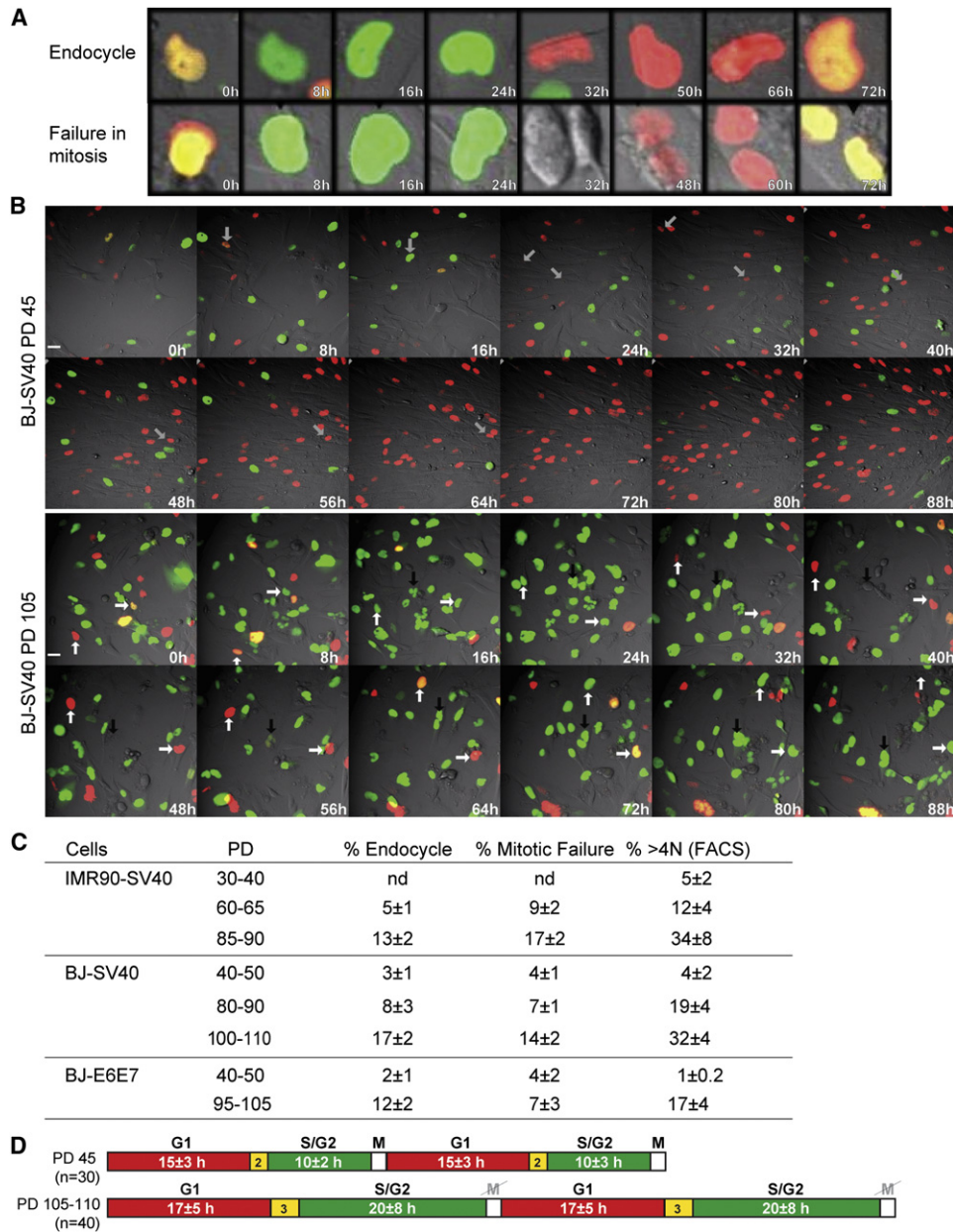
Figure 3. Endoreduplication and Mitotic Failure in Telomere Crisis

(A and B) FUCCI live-cell imaging of BJ-SV40 cells at PD45 and PD105 analyzed by time-lapse every 20 min for 96 hr. (A) Enlarged images exemplifying endoreduplication and mitotic failure. (B) Selected time points from Movie S1. Arrows with the same orientation highlight the same cell over time. In BJ-SV40 PD 45, the arrow highlights one cell progressing through a normal cell cycle. In BJ-SV40 cells PD 105, the white arrows highlight two cells undergoing endoreduplication; the black arrow highlights mitotic failure. Scale bar = 20 μm.

(C) Table summarizing the data derived from FUCCI imaging as in (B) (Movies S1 and S2) and FACS of BJ-SV40, IMR90-SV40, and BJ-E6E7. The average and SD obtained from three independent experiments is given (n is the total number of cells analyzed in each case).

(D) BJ-SV40 cells at the indicated PDs were imaged as in (A). The indicated number of cells was followed during the imaging session and the duration (hours) of the presence of geminin and Cdt1 was analyzed (average values are indicated).

See also Figure S3 and Movies S1 and S2.

or extensive replicative telomere shortening (PD 70–80; Figures 5A–5C; Figures S4A–S4C). As compared to PD 30, at PD 70–80 the BJ-p53 dn cells showed a small increase in the fraction of tetraploid cells (<1% to ~7%) (Figures 5A and 5B). The DNA damage response was active in BJ-p53 dn cells at PD 70–80, as shown by Chk1 phosphorylation and an increased number of 53BP1 foci compared to earlier PDs (Figure 5C; Figure S4C). FACS analysis indicated that BJ-p53dn showed fewer tetraploid cells and a lower fraction of cells in G2 compared to BJ-SV40 at the same PD (Figures 1E, 5A, and 5B). Furthermore, after 96 hr of zeocin treatment, only ~9% of BJ-p53dn cells had a DNA content >4N (Figures 5A and 5B), whereas 20%–25% of
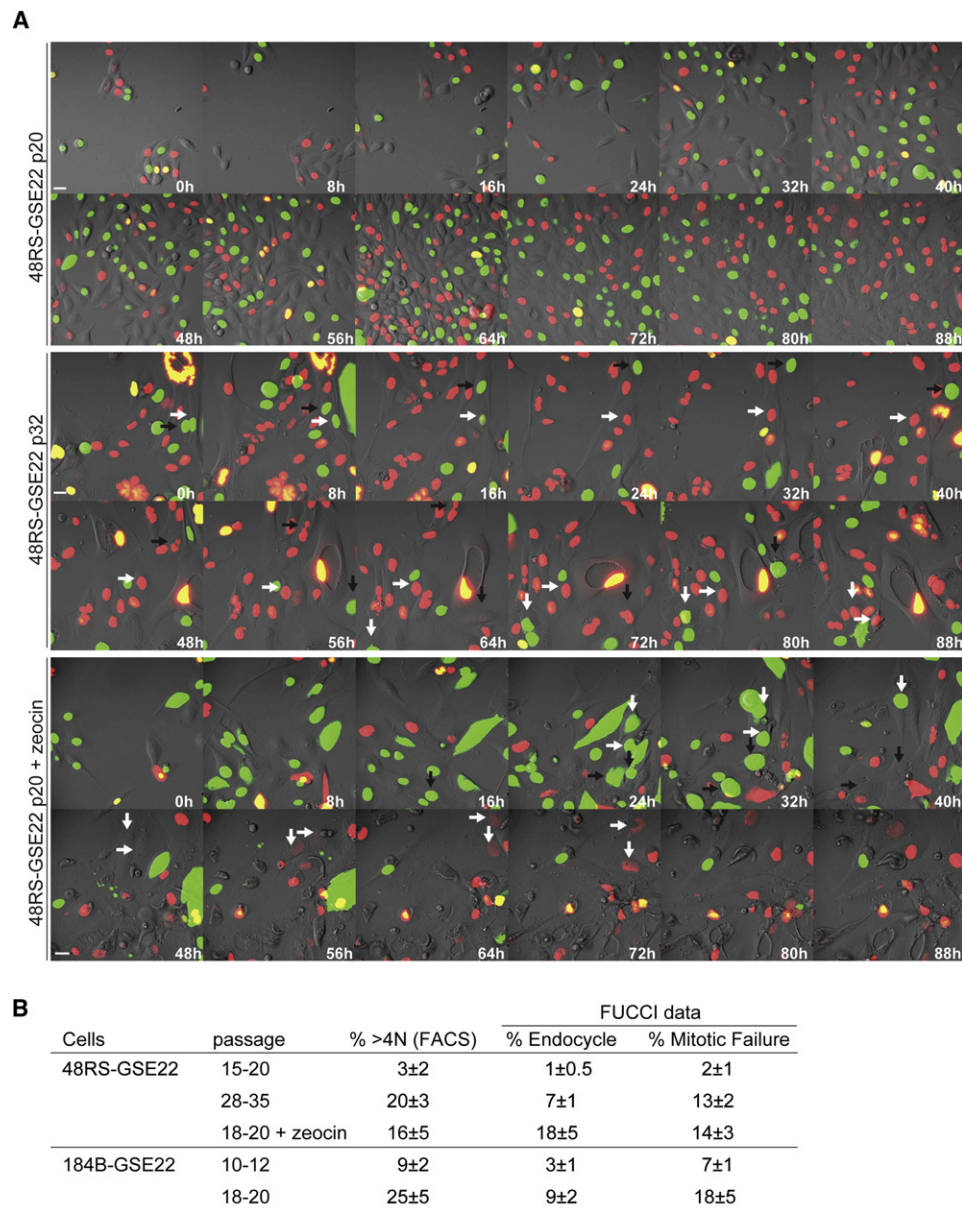
Figure 4. Endoreduplication and Mitotic Failure in hMECs in Telomere Crisis

(A) FUCCI imaging (as in Figures 3A and 3B) of 48RS-GSE22 at the indicated passages with or without zeocin treatment. Indicated time points are from Movie S3. Arrows with the same orientation highlight the same cell over time. In 48RS-GSE22 p32 and p20+zeocin, the white arrows highlight cells showing endoreduplication and the black arrows highlight cells undergoing mitotic failure. Scale bar = 20 μm.

(B) Table summarizing data derived from FUCCI imaging (Movie S3) and FACS (as in Figure 3C).

See also Figure S2 and Movie S3.

BJ-SV40 became tetraploid after zeocin treatment (Figures 5A and 5B; Davoli et al., 2010). Similar data were obtained using IMR90 and RPE (retinal pigment epithelial) cells lacking p53 function (Figures S4D and S4E and data not shown), whereas tetraploidy was not induced in primary RPE and BJ cells, which arrested in G1/S (Figures S4D and S4E and data not shown). Consistent with a role of the Rb pathway in mediating a G1/S arrest in response to telomere and genome-wide DNA damage, the level of p16 increased at increasing PDs and after zeocin treatment (Figure 5C). These data suggest that the activa-

tion of the Rb/p16 pathway contributes to the repression of tetraploidization in cells experiencing a persistent DNA damage response.

The low level of residual tetraploidization in the Rb-proficient cells could be explained if the Rb pathway led to a block in G1 but not in G2. We therefore isolated FACS-sorted G1 and S/G2 cells, subjected them to zeocin treatment soon after plating, and then used FUCCI imaging to determine their tendency to undergo cell cycle progression and/or tetraploidization. Approximately 60% of the G1-sorted BJ-p53dn cells treated with
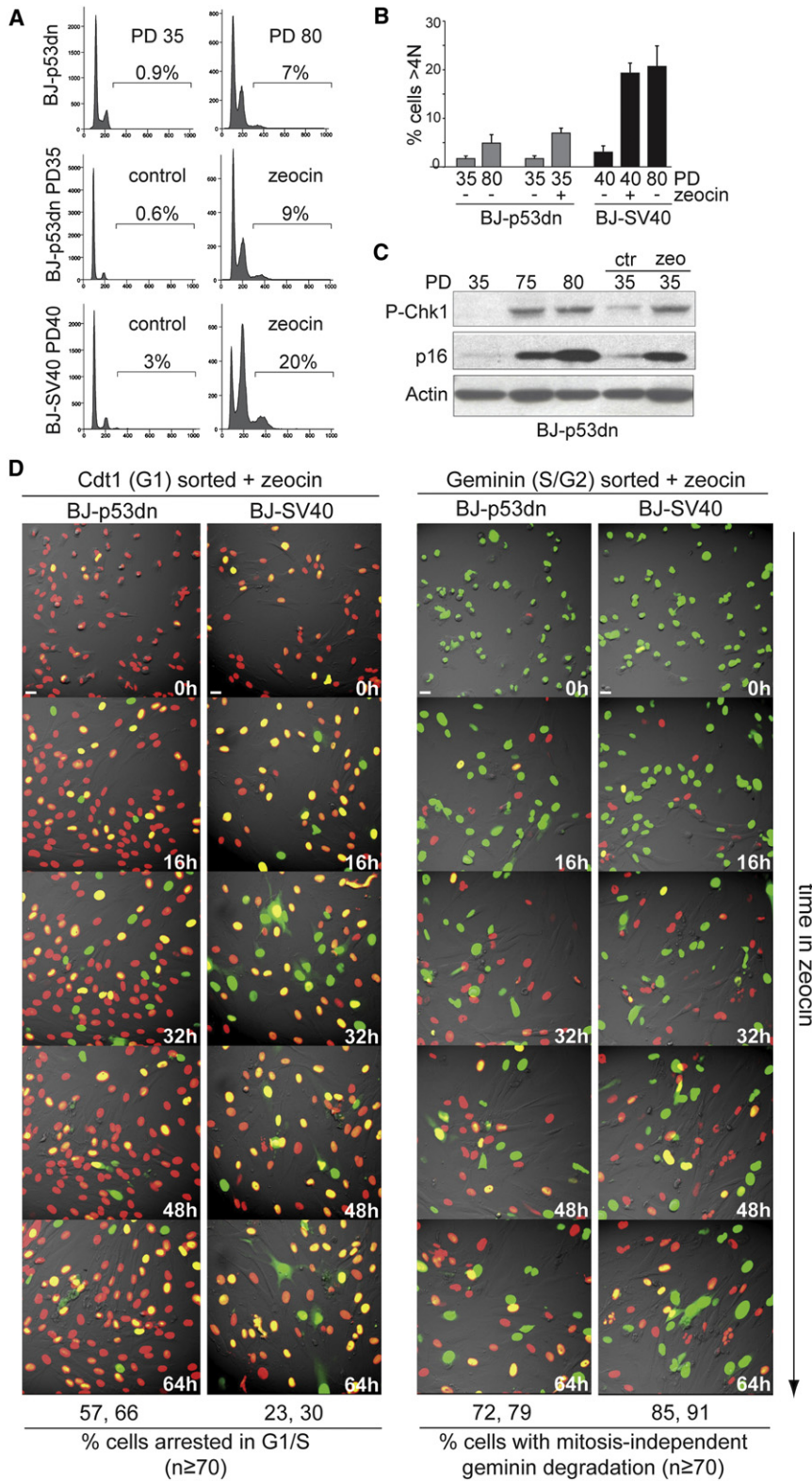
in G1/S after zeocin treatment (Figure 5D; Movie S4). In contrast, approximately 75% of the BJ-p53dn S/G2 cells underwent endoreduplication, showing mitosis-independent geminin degradation and re-entry into G1 and S-phase (Figure 5D; Movie S5). BJ-SV40 cells in S/G2 showed the same percentage of endoreduplication, indicating that Rb status does not affect tetraploidization of cells experiencing prolonged DNA damage in S/G2. Although we cannot exclude other aspects of SV40 large T antigen expression, these data suggest that activation of the Rb/p16 pathway blocks entry into S phase in cells that experience a DNA damage signal in G1, thereby limiting the occurrence of tetraploidization. In contrast, the Rb/p16 pathway alone is not capable of preventing endoreduplication when the DNA damage takes place in G2.

Telomere-Driven Tetraploidization Promotes Transformation in Mouse Cells

To address the tumorigenic potential of tetraploidization, we used an inducible system to elicit transient telomere dysfunction, mimicking the temporary loss of telomere protection that is thought to occur early in tumorigenesis before telomerase activation. We employed the previously established tet-OFF inducible system for POT1a expression in MEFs expressing SV40-LT (Davoli et al., 2010). Two POT1a-tetOFF cell

zeocin remained in G1/S phase of the cell cycle (red or yellow) throughout the 96 hr imaging session (Figure 5D; Movie S4) whereas only 25%–30% of G1-sorted BJ-SV40 cells arrested
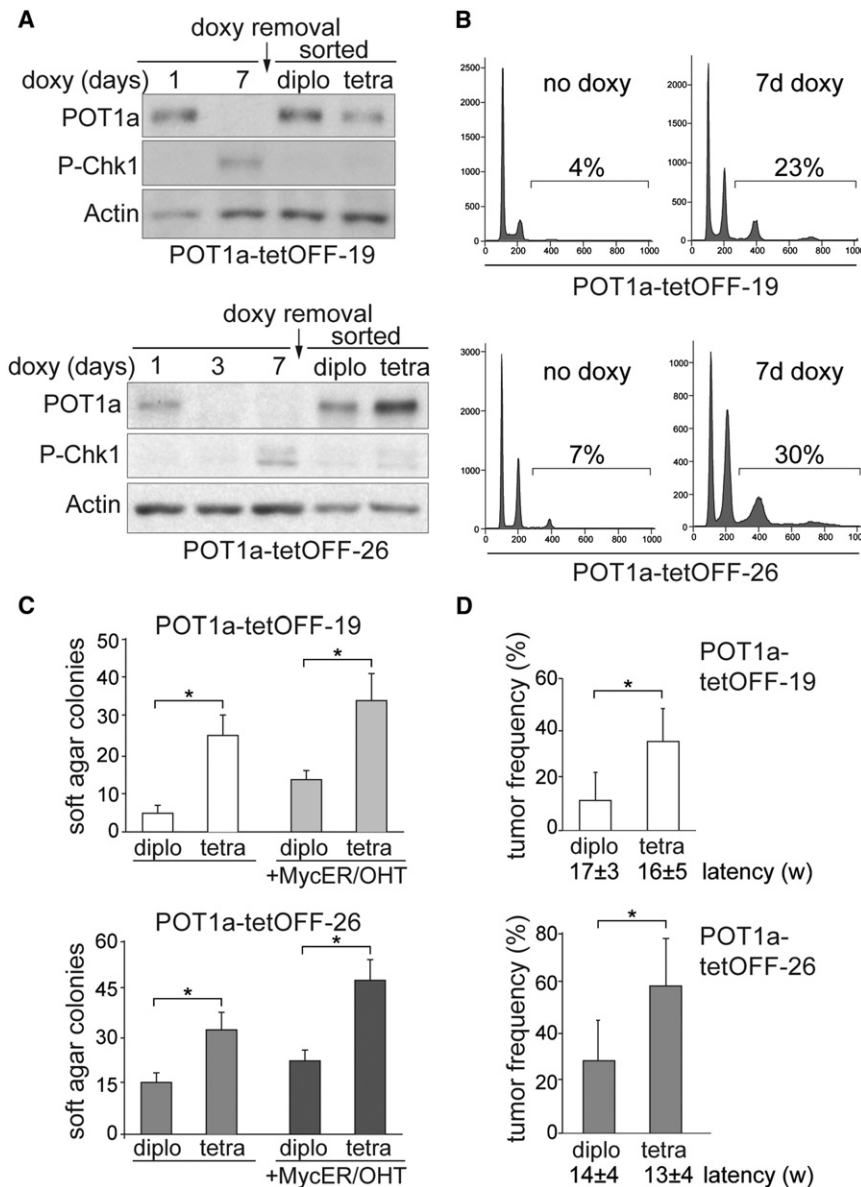
Figure 6. Telomere-Driven Tetraploidy Promotes Cellular Transformation in Mouse Cells

(A) Immunoblot for Chk1 phosphorylation and POT1a in POT1a-tetOFF-19 and -26 cells (SV40-LT expressing MEFs) at the indicated time after treatment with doxycycline and after release of the FACS-sorted diploid and tetraploid cells. POT1a-tetOFF clones 19 and 26 (Davoli et al., 2010) were treated with doxycycline for 10 days, FACS sorted after Hoechst 33342 staining, and cultured in the absence of doxycycline.

(B) FACS analysis of POT1a-tetOFF-19 and -26 treated as in (A). The percentage of cells with >4N DNA content is indicated.

(C) POT1a-tetOFF-19 and -26 with or without pBabe-Myc-ER were treated as in (A). FACS sorted diploid and tetraploid cells were expanded for 2 weeks or for 6–8 weeks and plated in soft-agar. The colonies were counted after 4–6 weeks. Myc-ER was induced with 0.5 μM OHT. The average number of colonies per well and SD obtained after 3 or 4 independent experiments is shown. Stars indicate statistically significant difference (p < 0.05 after paired Student's t test, Prism 5 software).

(D) Tumorigenicity assay in nude mice. Diploid and tetraploid descendants of POT1a-tetOFF-19 and-26 were expanded for 2 weeks or for 5–6 weeks in culture in the absence of doxycycline subcutaneously injected in nude mice (2.5 or 5 10^5 cells injected on each side; the number of injected mice is shown). The average frequencies of tumor formation and latencies are indicated with standard deviation (three or four experiments, five or ten mice per experiment). Stars indicate a statistically significant difference (p < 0.05 after paired Student's t test).

See also Figure S5.

lines were derived (POT1atetOFF-19 and -26) in which treatment with doxycycline transiently depletes POT1a. As expected from previous data, the loss of POT1a was accompanied by the accumulation of 53BP1 at telomeres, phosphorylation of Chk1 (Figures 6A and 6B; Figure S5A) and tetraploidization as measured by FACS (Figure 6B). Tetraploidization was also evident in these cells from the supernumerary centrosomes and telomere clustering in interphase which are consistent with chromosome reduplication without chromosome segregation (Hockemeyer et al., 2006; Figures S5A and S5B). After doxycycline treatment, POT1a-tetOFF-19 and -26 cells were FACS-sorted based on Hoechst-staining for DNA content to derive tetraploid and diploid cells (Figure S5C). The diploid and tetraploid cells were cultured for either 2 or 5–6 weeks in the absence of doxycycline, allowing POT1a re-expression (Figure 6A). The results at these two time points were essentially the same.

The resulting diploid and tetraploid cultures were then tested for their ability to form colonies in soft-agar and tumors in nude mice (Figures 6C and 6D). For both POT1a-tetOFF-19 and -26, the tetraploid descendants were more transformed based on both assays. The transformation efficiency after long-term culture (5–6 weeks) was slightly higher than the one after short-term culture (2 weeks). Overexpression of c-Myc further enhanced the transformation of diploid and tetraploid POT1a-tetOFF cells but even without this oncogene, the greater tumorigenic potential of the tetraploid population was significant (Figures 6C and 6D). POT1atetOFF control cells not treated with doxycycline transformed at a rate similar to the sorted diploid cells (not shown). The increased transformation potential in the tetraploid cells was not due to increased proliferation rate, since the tetraploid cells grew slower than their diploid counterparts (Figure S5D).

Evolution of Subtetraploid Karyotypes

In order to monitor the karyotypic changes during tumor outgrowth, we established cell lines from tumors formed upon injection of diploid and tetraploid mouse cells. Prior to injection

into nude mice, the cells were infected with the histone H2B-GFP construct allowing separation of tumor cells from host-derived cells present in the tumor mass. GFP-positive cells of tumors derived from injected tetraploid cells showed a tetraploid-like profile, consistent with their cells of origin (Figures S5E and S5F). As expected, the host-derived GFP-negative cells showed a diploid-like profile. A total of eight GFP-positive cell lines were derived from tumors formed by the POT1a-tetOFF-19 and -26 tetraploid cells. Their chromosome numbers, determined after propagation of the cells for 7–10 days in culture revealed subtetraploid karyotypes, with the exception of one line which was hyper-tetraploid (chromosome number ~120, Figures 7A and 7B). Evolution of subtetraploid karyotypes had also occurred in three of four cell lines derived from soft-agar colonies formed by tetraploid POT1a-tetOFF-26 cells (Figure 7C). As a control, cell lines established from a soft-agar colony and a tumor formed by diploid cells had a near-diploid karyotype (Figures 7B and 7C). These results indicate that tetraploid cells generated through telomere dysfunction have a high rate of chromosome loss.

DISCUSSION

Here, we show that telomere crisis induces tetraploidization in human fibroblasts and mammary epithelial cells, lending further credence to the role of telomeres in shaping cancer genomes. Telomere dysfunction has long been held responsible for the initiation of breakage-fusion-bridge cycles and their accompanying rearrangements, including nonreciprocal translocations, regional amplifications, and segmental deletions. The finding that tetraploidization is an additional corollary of unmitigated telomere attrition adds to this inventory of telomere-related genome instability and provides a framework for the genesis of human tumors carrying heavily rearranged subtetraploid genomes. Among the potentially pervasive sources of genome instability in cancer, which include rearrangements originating from common fragile sites, chromothrypsis, and deficiencies in double-strand break repair (Durkin and Glover, 2007; Harper and Elledge, 2007; Negrini et al., 2010; Stephens et al., 2011), an episode of telomere dysfunction stands out, however, due its potential aggregate effect. Upon activation of telomerase, the cells emerging from telomere crisis could potentially combine the mutator phenotype of breakage-fusion-bridge cycles, the mutational robustness of a tetraploid genome, and the high chromosome missegregation rate associated with supernumary centrosomes.

Although we had previously used mouse embryo fibroblasts to document endoreduplication after removal of POT1a from mouse telomeres, it was unclear whether the resulting telomere dysfunction resembles the molecular events at telomeres that have become too short after prolonged attrition. For instance, removal of POT1a from mouse telomeres exposes the single-stranded DNA and permanently activates the ATR kinase pathway whereas critically shortened telomeres may be expected to lose several (or all) shelterin proteins rather than POT1 alone and are known to activate both ATM and ATR signaling (d'Adda di Fagagna et al., 2003). It is also unlikely that all telomeres in crisis cells become dysfunctional at the same time so that the overall level of the DNA damage signal elicited by telomere crisis might be less than in the POT1a knockout cells.
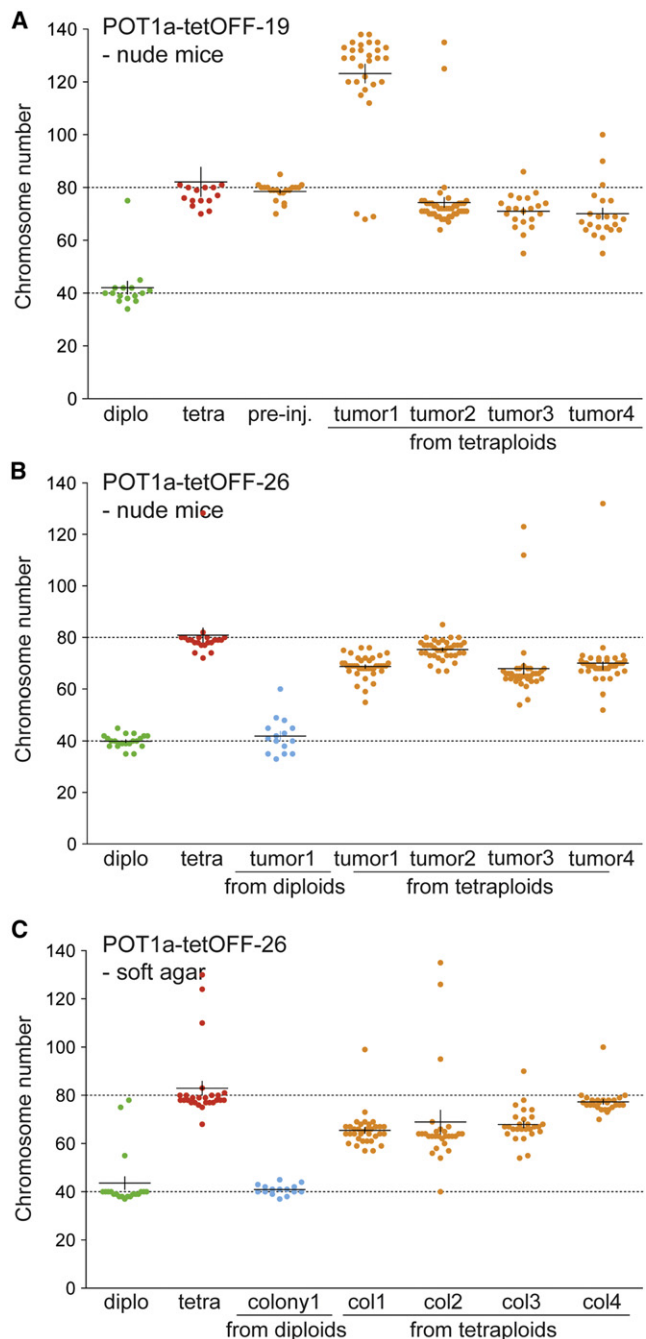

Figure 7. Evolution of Subtetraploid Karyotypes

(A and B) Graphs indicating the number of chromosomes/metaphase in cells derived from tumors formed by diploid and tetraploid POT1a-tetOFF-19 and -26 cells (as in Figure 6D). Cell lines were derived from tumors and metaphase spreads were analyzed after 7–10 days. The distribution of the chromosome number of POT1a-tetOFF diploid and tetraploid cells before injection and of cell lines derived from the indicated tumors derived from injected diploid or tetraploid cells is shown.

(C) Graphs indicating the number of chromosomes/metaphase in cells derived from soft-agar colonies formed POT1a-tetOFF-26 (as in Figure 6D).

Furthermore, rather than the irreparable damage at all telomeres generated by POT1a deletion, critically shortened telomeres are repaired by NHEJ and the resulting damage signal at each telomere is therefore transient. The current data now clarify these issues and demonstrate that endoreduplication can be induced by the DNA damage response to shortened telomeres as they occur in cells in crisis. Furthermore, the data argue that this pathway is similar in human and mouse cells, despite the distinctions in their telomere damage response pathways (Smogorzewska and de Lange, 2002; Jacobs and de Lange, 2004), and demonstrate the relevance of telomere-driven tetraploidization in epithelial cells, which are a cancer relevant cell type.

The data indicate that tetraploid mouse cells generated telomere-driven tetraploidization are more tumorigenic than their diploid counterparts. This result is consistent with prior work showing a higher tumorigenic potential of tetraploid cells generated through the use of a cytokinesis inhibitor (Fujiwara et al., 2005). In the case of telomere-driven tetraploidization there is no prolonged arrest in mitosis, no binucleate intermediate is formed, and there is no reorganization of the two chromosome sets into a tetraploid genome in the next mitosis. Our findings therefore indicate that the tetraploidization per se is the most likely source of the greater tumorigenic potential of the cells.

Order of Events

Telomere-dependent tetraploidization requires a precise sequence of events during tumorigenesis. Specifically, both the p53 and Rb pathways have to be inactivated and the telomeres have to become sufficiently short to induce telomere crisis before telomerase is activated. Loss of p53 is required for the by-pass of telomere-driven senescence and is well-established as a prerequisite for the proliferation of tetraploid cells (Margolis et al., 2003; Ganem et al., 2007). The Rb pathway also blocks cell cycle progression in response to telomere dysfunction and thereby curbs the emergence and proliferation of tetraploid descendants (Jacobs and de Lange, 2004). For most human tumors, there is limited information of the exact order of events relevant to telomere-driven tetraploidization. In particular, no prior study has examined indices of tetraploidization, changes in the status of p53/Rb, and telomerase expression in the same set of pathological specimen representing different stages in tumorigenesis. However, for a number of tumor types, it is known that tetraploidization arises at a stage when both p53 and Rb become inactivated and telomerase is not yet active (Davoli and de Lange, 2011). Examples include HPV induced cervical carcinoma, bladder cancer, lung cancer, breast cancer, and colon cancer. Breast cancer represents a particularly interesting case because there is good evidence for loss of Rb and p53, telomere crisis, and tetraploidization in DCIS before telomerase is activated (Shay and Bacchetti, 1997; Chin et al., 2004; Ottesen, 2003; Shackney and Silverman, 2003). On the other hand, there are also several tumor types that express high levels of telomerase at an early stage (e.g., certain leukemias and lymphomas) and are therefore unlikely to experience telomere crisis. Perhaps not surprisingly, these tumors lack the frequent rearrangements that scar the genomes of solid human tumors and are mostly near diploid.

Collectively, these data suggest a general mechanism for tetraploidization in the early stages of human tumorigenesis. When the p53 and Rb pathway are inactive, extreme telomere shortening can induce tetraploidization through endoreduplication or mitotic failure in precancerous lesions. Reactivation of telomerase (or other mechanisms of telomere maintenance) will allow the tetraploid clone to expand and evolve into a fully transformed cancerous state. The chromosome instability due to prior telomere dysfunction and the inherent high rate of chromosome mis-segregation of tetraploid cells may then foster the evolution of a profoundly rearranged subtetraploid cancer karyotype.

EXPERIMENTAL PROCEDURES

Cell Culture Procedure and Viral Gene Delivery

BJ (ATCC#: CRL2522) and IMR90 (ATCC#: CCl186) human fibroblasts were transduced with retroviral vectors expressing SV40-LT, HPV-E6/E7, or p53175H (p53 dn) as described in (Karlseder et al., 2002; Jacobs and de Lange, 2004). RPE human retinal pigment epithelial cells were purchased from ATCC (ATCC#: 2302) and retrovirally infected with pLPC-Puro-SV40-LT or pRetro-Super-Hygro-p53sh vectors. Human mammary epithelial cell lines 184B and 48RS (Romanov et al., 2001), expressing or not the GSE22 peptide (GSE), acting as a p53 dominant negative (Garbe et al., 2007) were kindly provided by Dr. Martha Stampfer. POT1a-tetOFF MEFs cell lines 19 and 26 were derived as described elsewhere (Davoli et al., 2010). POT1a-tetOFF MEFs, IMR90, BJ, and RPE cells were grown in DMEM (containing 10% of Medium 199 in the case of BJ cells) supplemented with 10% FBS, 100 U penicillin, 0.1 mg/ml streptomycin, 2 mM L-glutamine. hMEC cells were grown in MEMG (Lonza) supplemented with isoproterenol (10 μM) and transferrin (5 μg/ml). Human cells were transduced with FUCCI lentiviral vectors expressing mKO2-hCdt1 (red) and mAG-hGeminin (green) (Sakaue-Sawano et al., 2008), generously provided by Dr. Atsushi Miyawaki. Dr. Pier Giuseppe Pelicci provided pBabe-Puro-MycER. For retroviral and lentiviral infections, phoenix cells (retro) or 293T (lenti) cells were transfected with 10–20 μg of the transgene-expressing plasmid (in addition to lentiviral packaging vectors in the case of 293T). Supernatants were used for two to four infections of 4–6 hr were performed starting 36 hr after transfection with addition of 2–4 μg/ml of polybrene. Cells were selected for 4–6 days in the presence of 500 ng/ml of puromycin or 200 μg/ml of hygromycin. Zeocin (Invitrogen, 100 μg/ml final concentration) and doxycycline (1–2 μg/ml) were added to the cell culture medium every 2–3 days.

FACS Analysis and FACS Sorting

DNA content was analyzed by FACS in ethanol-fixed after staining with propidium iodide (PI), using standard procedures. Flow cytometry was performed using the FACScalibur (Becton Dickinson) and data were analyzed using FlowJo 8.7.1 software. To calculate the percentage of polyploid cells (DNA content >4N), cell doublets and sub-G1 apoptotic cells were excluded. Diploid and tetraploid cells were isolated by sorting for a G1 diploid DNA content or a G2 tetraploid DNA content using an BD FACSAria-2 cell sorter (BD Biosciences) after incubation with Hoechst 33342 (10 μM, AnaSpec, Inc.) for 30 min. GFP-positive cells expressing H2B-GFP were sorted using the same instrument.

In Vitro and In Vivo Transformation Assay

For in vitro soft-agar colony forming assay, a bottom layer of 2 ml 0.9% agar in medium was prepared and allow to solidify and cells were seeded in a top layer of 0.45% agar in medium at a density of 10^4 cells per well in 6-well dishes (triplicates were made for each cell line in each experiment). Cells were incubated at 37°C (medium was added periodically) and colonies formed after 4–6 weeks were scored. In the indicated cases, 0.5 nM 4-hydroxytamoxifen (4-OHT, Sigma) was added to the top layer. In vivo tumorigenic assay was performed by subcutaneous injection in nude mice. Diploid or tetraploid POT1a-tetOFF-19 or -26 cells (5×10^5) were resuspended in PBS and injected into the contra-lateral sides of NCR-*Foxn1*$^{nu/nu}$ female mice (Taconic). The recipient mice were

checked once or twice a week for tumor formation and euthanized when tumors reached 1 cm diameter, in accordance with institutional procedures. Tumors were dissociated into single cells by treatment with collagenase A at 250 units/ml in DMEM for 3 hr at 37°C. Cells were then washed repeatedly and plated in 10 cm dishes. All experiments involving mice were performed in accordance with institutional regulations and ethical guidelines, and have been authorized by the Institutional Animal Care and Use Committee at Rockefeller University.

Immunofluorescence, Fluorescence In Situ Hybridization-Immunofluorescence, and Immunoblotting

Immunofluorescence (IF) and fluorescence in situ hybridization (FISH)-IF on coverslips and telomeric FISH on metaphase spreads were performed as described previously (Celli and de Lange, 2005). Briefly, after fixation, cells on coverslips were blocked in for 30 min in blocking solution (PBS with 0.1% Triton X-100, 1 mM EDTA, 3% goat serum, and 1 mg/ml BSA). Cells were then incubated for 1 hr with primary antibody diluted in blocking solution (anti-53BP1, 100-304-A, Novus Biologicals; anti-centrin2, sc-27793-R, Santa Cruz), washed three times in PBS and incubated with Rhodamine Red-X or Alexa Fluor 488 conjugated secondary antibody. Finally cells were washed in PBS and the DNA was counterstained with DAPI. In the case of IF-FISH or FISH on metaphase spreads, cells or slides with metaphases were dehydrated in ethanol and hybridized with PNA-probe FITC-OO-(AATCCC)3 (Applied Biosystems) in hybridizing solution (70% formamide, 10 mM Tris-HCl [pH 7.2], 1 mg/ml blocking reagent [Roche]). After denaturation (10 min at 80°C), hybridization was performed at room temperature for 2 hr, followed by two washes for 15 min with washing solution (70% formamide, 10 mM Tris-HCl [pH 7.2]). Finally cells or metaphase spreads were washed in PBS and DNA was then counterstained with DAPI. Digital images were captured with a Zeiss Axioplan II microscope using Improvision OpenLab software. Immunoblotting was performed as described in (Celli and de Lange, 2005) with the following antibodies were used: Chk2 (611570, BD Biosciences); Chk1, P-S317 (A300-163A, Bethyl) for human cells; Chk1 pS345 (#2348, Cell Signaling Technology) for mouse cells; β-actin (I-19) (sc-1616, Santa Cruz); p16 (C-20) (Santa Cruz); POT1a (1221).

Telomere Length Analysis

For genomic blotting, cells were harvested at the indicated PD, DNA was isolated as described (de Lange et al., 1990), digested with AluI and MboI, size-fractionated on a 0.7% agarose gel and transferred to a Hybond membrane for hybridization using an 800 bp telomeric DNA probe from pSP73Sty11 labeled with [CCCTAA]3-primed Klenow polymerase and ^{32}P-alpha-dCTP. Blots were exposed to a phosphorimaging screen and analyzed using Image-Quant software.

REFERENCES

Arias, E.E., and Walter, J.C. (2005). Replication-dependent destruction of Cdt1 limits DNA replication to a single round per cell cycle in Xenopus egg extracts. Genes Dev. 19, 114–126.

Artandi, S.E., and DePinho, R.A. (2010). Telomeres and telomerase in cancer. Carcinogenesis 31, 9–18.

Artandi, S.E., Chang, S., Lee, S.L., Alson, S., Gottlieb, G.J., Chin, L., and DePinho, R.A. (2000). Telomere dysfunction promotes non-reciprocal translocations and epithelial cancers in mice. Nature 406, 641–645.

Baker, S.J., Preisinger, A.C., Jessup, J.M., Paraskeva, C., Markowitz, S., Willson, J.K., Hamilton, S., and Vogelstein, B. (1990). p53 gene mutations occur in combination with 17p allelic deletions as late events in colorectal tumorigenesis. Cancer Res. 50, 7717–7722.

Celli, G.B., and de Lange, T. (2005). DNA processing is not required for ATM-mediated telomere damage response after TRF2 deletion. Nat. Cell Biol. 7, 712–718.

Chin, K., de Solorzano, C.O., Knowles, D., Jones, A., Chou, W., Rodriguez, E.G., Kuo, W.L., Ljung, B.M., Chew, K., Myambo, K., et al. (2004). In situ analyses of genome instability in breast cancer. Nat. Genet. 36, 984–988.

Counter, C.M., Avilion, A.A., LeFeuvre, C.E., Stewart, N.G., Greider, C.W., Harley, C.B., and Bacchetti, S. (1992). Telomere shortening associated with chromosome instability is arrested in immortal cells which express telomerase activity. EMBO J. 11, 1921–1929.

d'Adda di Fagagna, F., Reaper, P.M., Clay-Farrace, L., Fiegler, H., Carr, P., Von Zglinicki, T., Saretzki, G., Carter, N.P., and Jackson, S.P. (2003). A DNA damage checkpoint response in telomere-initiated senescence. Nature 426, 194–198.

Davoli, T., and de Lange, T. (2011). The causes and consequences of polyploidy in normal development and cancer. Annu. Rev. Cell Dev. Biol. 27, 22.1–22.26.

Davoli, T., Denchi, E.L., and de Lange, T. (2010). Persistent telomere damage induces bypass of mitosis and tetraploidy. Cell 141, 81–93.

de Lange, T. (2005). Telomere-related genome instability in cancer. Cold Spring Harb. Symp. Quant. Biol. 70, 197–204.

de Lange, T., Shiue, L., Myers, R.M., Cox, D.R., Naylor, S.L., Killery, A.M., and Varmus, H.E. (1990). Structure and variability of human chromosome ends. Mol. Cell. Biol. 10, 518–527.

Durkin, S.G., and Glover, T.W. (2007). Chromosome fragile sites. Annu. Rev. Genet. 41, 169–192.

Fujiwara, T., Bandi, M., Nitta, M., Ivanova, E.V., Bronson, R.T., and Pellman, D. (2005). Cytokinesis failure generating tetraploids promotes tumorigenesis in p53-null cells. Nature 437, 1043–1047.

Ganem, N.J., Storchova, Z., and Pellman, D. (2007). Tetraploidy, aneuploidy and cancer. Curr. Opin. Genet. Dev. 17, 157–162.

Garbe, J.C., Holst, C.R., Bassett, E., Tlsty, T., and Stampfer, M.R. (2007). Inactivation of p53 function in cultured human mammary epithelial cells turns the telomere-length dependent senescence barrier from agonescence into crisis. Cell Cycle 6, 1927–1936.

Harper, J.W., and Elledge, S.J. (2007). The DNA damage response: ten years after. Mol. Cell 28, 739–745.

Hastie, N.D., Dempster, M., Dunlop, M.G., Thompson, A.M., Green, D.K., and Allshire, R.C. (1990). Telomere reduction in human colorectal carcinoma and with ageing. Nature 346, 866–868.

Herbig, U., Jobling, W.A., Chen, B.P., Chen, D.J., and Sedivy, J.M. (2004). Telomere shortening triggers senescence of human cells through a pathway involving ATM, p53, and p21(CIP1), but not p16(INK4a). Mol. Cell 14, 501–513.

Hockemeyer, D., Daniels, J.P., Takai, H., and de Lange, T. (2006). Recent expansion of the telomeric complex in rodents: Two distinct POT1 proteins protect mouse telomeres. Cell 126, 63–77.

Jacobs, J.J., and de Lange, T. (2004). Significant role for p16INK4a in p53-independent telomere-directed senescence. Curr. Biol. 14, 2302–2308.

Karlseder, J., Smogorzewska, A., and de Lange, T. (2002). Senescence induced by altered telomere state, not telomere loss. Science 295, 2446–2449.

Kibe, T., Osawa, G.A., Keegan, C.E., and de Lange, T. (2010). Telomere protection by TPP1 is mediated by POT1a and POT1b. Mol. Cell. Biol. 30, 1059–1066.

Kim, N.W., Piatyszek, M.A., Prowse, K.R., Harley, C.B., West, M.D., Ho, P.L., Coviello, G.M., Wright, W.E., Weinrich, S.L., and Shay, J.W. (1994). Specific association of human telomerase activity with immortal cells and cancer. Science 266, 2011–2015.

Kirkland, J.A., Stanley, M.A., and Cellier, K.M. (1967). Comparative study of histologic and chromosomal abnormalities in cervical neoplasia. Cancer 20, 1934–1952.

Lengauer, C., Kinzler, K.W., and Vogelstein, B. (1997). Genetic instability in colorectal cancers. Nature 386, 623–627.

Lin, T.T., Letsolo, B.T., Jones, R.E., Rowson, J., Pratt, G., Hewamana, S., Fegan, C., Pepper, C., and Baird, D.M. (2010). Telomere dysfunction and fusion during the progression of chronic lymphocytic leukemia: evidence for a telomere crisis. Blood 116, 1899–1907.

Margolis, R.L., Lohez, O.D., and Andreassen, P.R. (2003). G1 tetraploidy checkpoint and the suppression of tumorigenesis. J. Cell. Biochem. 88, 673–683.

Meeker, A.K., and Argani, P. (2004). Telomere shortening occurs early during breast tumorigenesis: a cause of chromosome destabilization underlying malignant transformation? J. Mammary Gland Biol. Neoplasia 9, 285–296.

Meeker, A.K., Hicks, J.L., Platz, E.A., March, G.E., Bennett, C.J., Delannoy, M.J., and De Marzo, A.M. (2002). Telomere shortening is an early somatic DNA alteration in human prostate tumorigenesis. Cancer Res. 62, 6405–6409.

Meeker, A.K., Hicks, J.L., Iacobuzio-Donahue, C.A., Montgomery, E.A., Westra, W.H., Chan, T.Y., Ronnett, B.M., and De Marzo, A.M. (2004). Telomere length abnormalities occur early in the initiation of epithelial carcinogenesis. Clin. Cancer Res. 10, 3317–3326.

Negrini, S., Gorgoulis, V.G., and Halazonetis, T.D. (2010). Genomic instability—an evolving hallmark of cancer. Nat. Rev. Mol. Cell Biol. 11, 220–228.

Ottesen, G.L. (2003). Carcinoma in situ of the female breast. A clinico-pathological, immunohistological, and DNA ploidy study. APMIS Suppl. 108, 1–67.

Reid, B.J., Barrett, M.T., Galipeau, P.C., Sanchez, C.A., Neshat, K., Cowan, D.S., and Levine, D.S. (1996). Barrett's esophagus: ordering the events that lead to cancer. Eur. J. Cancer Prev. 5 (Suppl 2), 57–65.

Remus, D., and Diffley, J.F. (2009). Eukaryotic DNA replication control: lock and load, then fire. Curr. Opin. Cell Biol. 21, 771–777.

Romanov, S.R., Kozakiewicz, B.K., Holst, C.R., Stampfer, M.R., Haupt, L.M., and Tlsty, T.D. (2001). Normal human mammary epithelial cells spontaneously escape senescence and acquire genomic changes. Nature 409, 633–637.

Sakaue-Sawano, A., Kurokawa, H., Morimura, T., Hanyu, A., Hama, H., Osawa, H., Kashiwagi, S., Fukami, K., Miyata, T., Miyoshi, H., et al. (2008). Visualizing spatiotemporal dynamics of multicellular cell-cycle progression. Cell 132, 487–498.

Shackney, S.E., and Silverman, J.F. (2003). Molecular evolutionary patterns in breast cancer. Adv. Anat. Pathol. 10, 278–290.

Shackney, S.E., Smith, C.A., Miller, B.W., Burholt, D.R., Murtha, K., Giles, H.R., Ketterer, D.M., and Pollice, A.A. (1989). Model for the genetic evolution of human solid tumors. Cancer Res. 49, 3344–3354.

Shay, J.W., and Bacchetti, S. (1997). A survey of telomerase activity in human cancer. Eur. J. Cancer 33, 787–791.

Shay, J.W., and Wright, W.E. (2005). Senescence and immortalization: role of telomeres and telomerase. Carcinogenesis 26, 867–874.

Shay, J.W., Pereira-Smith, O.M., and Wright, W.E. (1991). A role for both RB and p53 in the regulation of human cellular senescence. Exp. Cell Res. 196, 33–39.

Shay, J.W., Van Der Haegen, B.A., Ying, Y., and Wright, W.E. (1993). The frequency of immortalization of human fibroblasts and mammary epithelial cells transfected with SV40 large T-antigen. Exp. Cell Res. 209, 45–52.

Smogorzewska, A., and de Lange, T. (2002). Different telomere damage signaling pathways in human and mouse cells. EMBO J. 21, 4338–4348.

Stephens, P.J., Greenman, C.D., Fu, B., Yang, F., Bignell, G.R., Mudie, L.J., Pleasance, E.D., Lau, K.W., Beare, D., Stebbings, L.A., et al. (2011). Massive genomic rearrangement acquired in a single catastrophic event during cancer development. Cell 144, 27–40.

Storchova, Z., and Kuffer, C. (2008). The consequences of tetraploidy and aneuploidy. J. Cell Sci. 121, 3859–3866.

van Heek, N.T., Meeker, A.K., Kern, S.E., Yeo, C.J., Lillemoe, K.D., Cameron, J.L., Offerhaus, G.J., Hicks, J.L., Wilentz, R.E., Goggins, M.G., et al. (2002). Telomere shortening is nearly universal in pancreatic intraepithelial neoplasia. Am. J. Pathol. 161, 1541–1547.

Wright, W.E., and Shay, J.W. (1992). The two-stage mechanism controlling cellular senescence and immortalization. Exp. Gerontol. 27, 383–389.